Synthesis and properties of glasses in the K_2O-SiO_2-Bi_2O_3-TiO_2 system and bismuth titanate ($Bi_4Ti_3O_{12}$) nano glass-ceramics thereof

Atiar Rahaman Molla . Anal Tarafder . Basudeb Karmakar*

Glass Science and Technology Section, Glass Division, Central Glass and Ceramic Research Institute (Council of Scientific and Industrial Research, CSIR), 196 Raja S. C. Mullick Road, Kolkata 700 032, India

Abstract Glasses were prepared by the melt-quench technique in the K_2O-SiO_2-Bi_2O_3-TiO_2 (KSBT) system and crystallized bismuth titanate, BiT ($Bi_4Ti_3O_{12}$) phase in it by controlled heat-treatment at various temperature and duration. Different physical, thermal, optical and third order susceptibility ($\chi 3$) of the glasses were evaluated and correlated with their composition. Systematic increase in refractive index (n) and $\chi 3$ with increase in BiT content is attributed to the combined effects of high polarization and ionic refraction of bismuth and titanium ions. Microstructural evaluation by FESEM shows the formation of polycrystalline spherical particles of 70-90 nm along with nano rods of average diameter of 85-90 nm after prolonged heat-treatment. A minor increase in dielectric constants (ε_r) has been observed with increase in polarizable components of BiT in the glasses whereas a sharp increase in ε_r in glass-ceramics is found to be caused by the formation of non-centrosymmetric and ferroelectric BiT nanocrystals in the glass matrix.

Keywords: Bismuth titanate, Glass ceramics, Ferroelectric properties, Nanocomposites, Dielectric properties, Optical properties,

* Corresponding author: Tel: +91-33-2473 3469; fax: +91-33-2473 0957

E-mail address: basudebk@cgcri.res.in (B. Karmakar)

Introduction

Demonstration of electro-optic effect in transparent glasses containing ferroelectric crystalline phases has enhanced the prospects of using electro-optic glasses and glass-ceramics for various non-linear optical (NLO) applications [1,2,3]. Up to now, two kinds of ferroelectric oxides have become recognized as candidate for the memory materials; one is lead zirconate titanate [4] (PZT) and other is bismuth layer-structured ferroelectrics such as $SrBi_2Ta_2O_9$ (SBT) and $Bi_4Ti_3O_{12}$ (BiT) [5]. Though PZT has favourable polarization property, its use has been restricted due to the presence of large amount of toxic lead. SBT, however, shows a relatively low remanent polarization (P_r, 7-10 $\mu C/cm^2$) compared to BiT (P_r, 20 $\mu C/cm^2$), leading to a difficulty in establishing high density ferroelectric memories using SBT [6]. Thus, novel Pb-free ferroelectric with a larger P_r are expected for next-generation high-density ferroelectric memories. Hence, bismuth titanate ($Bi_4Ti_3O_{12}$, BiT), an n=3 member of the Aurivillius [7] family, is a promising candidate material for electro optic device applications. More than fifty ferroelectrics belong to the $Bi_4Ti_3O_{12}$ family, and all consist of Bi_2O_2 layers interleaved with perovskite-like $M_{n-1}R_nO_{3n+1}$ layer. Its crystal system is orthorhombic and unit cell parameters are 5.44, 32.815 and 5.41 for a, b and c axis. Newnham and co-workers [8] has established that distortions in crystal structure are responsible for the ferroelectricity of this family of materials. BiT is a high temperature ferroelectric ceramic ($T_c = 675^0C$) with useful properties for optical memory, piezoelectric and electro-optic devices [9]. In 1990s it became a key material for ferroelectric random access memory [10]. Though BiT ceramics are studied for this purpose, but one of the major difficulties of ceramics in piezoelectric applications is their high electrical conductivity, which interferes with the poling process [11] and also microstructure play a

critical role in the electrical properties, being the electrical conductivity dependent on the aspect ratio of grains [12] which makes processing of ceramics difficult to fabricate useful materials [13]. In this study, $Bi_4Ti_3O_{12}$ has been selected as ferroelectric phase because Bi^{3+} as a trivalent cation does not contribute to high ionic conductivity [14].

The glass-ceramic route of preparing bismuth titanate is desirable in order to obtain the material associated with pore free fine grained nano/microstructure embedded in a low permittivity, high resistivity host glass matrix [15]. Further, the interesting feature about this method is that it is possible to have a strict control over the crystallite size to the extent that transparent characteristics of the host glass is retained by crystallization [16]. For the last four decades since, after the remarkable discovery of Aurivillius [7] of a new family of material named after his name, a concerted effort by the researchers resulted in discovery of various novel glass-ceramics containing ferroelectric crystals such as BiT, (Na, K)NbO_3, $BaTiO_3$ [17,18,], $Pb_5Ge_3O_{11}$ [19], $LiNbO_3$ [20,21] $Bi_2VO_{5.5}$ [22], Bi_2WO_6 [15], Bi_2GeO_5 [23], solid solutions of $Pb_xBa_{1-x}TiO_3$ [24], $SrAl_2Si_2O_8$ [25] etc. embedded in a glass matrix.

Shankar and Varma [26] reported glass nanocomposites comprising nanocrystallites of bismuth titanate (BiT), dispersed in a glass matrix of strontium tetraborate SrB_4O_7 (SBO) by the controlled crystallization of glasses. They observed that ultrasonic treatment (UST) of the glass samples with an aqueous suspension of BiT followed by conventional heat treatment (HT) yielded the desired crystalline phase, which was otherwise difficult to obtain by conventional heat treatment. Gerth and Rüssel [27] have reported the crystallization of BiT in the Bi_2O_3-TiO_2-B_2O_3 system. However, they have observed the tendency of spontaneous devitrification and only samples with thickness of only ~1 mm could be produced with the system by employing cooling rate as high as ~500 K/min

during casting of glass melt. Kojima et al [10] prepared BiT glass-ceramics by a twin roller rapid quenching technique. However, synthesis and properties of K_2O-SiO_2-Bi_2O_3-TiO_2 glasses and bismuth titanate ($Bi_4Ti_3O_{12}$) crystal containing nano glass-ceramics in the K_2O-SiO_2-Bi_2O_3-TiO_2 system have not been reported elsewhere.

In view of the above facts, here we report the fabrication of K_2O-SiO_2-Bi_2O_3-TiO_2 glasses in the silicate matrix by the simple conventional melt-quenching technique followed by controlled heat-treatment to obtain bismuth titanate crystal containing glass-ceramic nanocomposites in bulk quantity. The focuses are on the thermal, structural, dielectric and optical properties evaluation of glasses as well as glass-ceramics with varying BiT content. Third order susceptibility of the glasses has also been evaluated. Properties of the glasses and glass-ceramics are correlated with their composition.

Experimental procedure

Six glasses with molar composition of (100-x) KS_2-xBiT (where KS_2 is potassium disilicate ($K_2O.2SiO_2$) and x = 10, 20, 30, 40, 45 and 50) and BiT corresponds to 2 Bi_2O_3. 3 TiO_2 ($Bi_4Ti_3O_{12}$) were prepared from high-purity chemicals of SiO_2 (99.8%, Sipur A1 Bremtheler Quartzitwerk, Usingen, Germany), potassium carbonate anhydrous, K_2CO_3 (GR, 99.9 %, Loba Chemie, Mumbai, India), titanium (IV) oxide, TiO_2 (99.3%, Merck KGaA, Darmstadt, Germany) and bismuth (III) oxide, Bi_2O_3 (99.0 %, Loba Chemie, Mumbai, India) by the conventional melt-quench technique. The samples have been designated as BiT10, BiT20, BiT30, BiT40, BiT45 and BiT50 respectively. About 50 g of glass batch was mixed thoroughly by agate-mortar and melted in a platinum crucible in an electric furnace at 1000-1150 ^{0}C for 2 h in air with intermittent stirring. The glass melt was

poured onto a preheated iron mould, followed by annealing at 465^0C for 2 h to remove the internal stresses of the glass, and then slowly cooled down @1^0C/min to room temperature. The as-prepared glass block was shaped into desired dimensions by cutting and optically polished to carry out various characterization experiments.

The refractive index of the precursor glass was measured by a Prism Coupler (Model 2010/M, Metricon Corporation, New Jersey, USA) at five different wavelengths of 473, 532, 632.8, 1064 and 1552 nm. As the coupling spot cannot be visible in infra red (IR) range, the sample was coupled with the prism at the same position in which it was coupled at 632.8 nm. During alignment of the lasers, special care was taken so that the alignments of 632.8, 1064 and 1552 nm lasers remain same. Further, these data have been used to estimate RI at other wavelengths employing Cauchy dispersion fittings. The resolution of the prism coupler is ±0.0005. DTA of precursor glass powders were carried out at temperatures up to 1000^0C at the rate of 10^0C/min with a NETZSCH instrument (Model STA 449 C, NETZSCH-Gerätebau GmbH, Germany). Glass transition temperature (T_g), co-efficient of thermal expansion (CTE) and deformation temperature (T_d) of the glass samples were evaluated using a horizontal dilatometer, NETZSCH DIL 402 PC (NETZSCH-Gerätebau GmbH, Germany). Softening temperature (T_s) was measured using glass softening point system (Model SP-3A, Harrop Industries Inc., OH, USA).

XRD data were recorded using an Xpert-Pro MPD diffractometer (PANalytical, Almelo, The Netherlands) with the Anchor Scan Parameters wavelength CuKa = 1.5406 Å at 25 ^{0}C, having a source power of 40 kV and 30 mA, in order to identify the developed crystalline phases of the glass–ceramics. A high-resolution FESEM (Gemini Zeiss Suprat 35 VP model of Carl Zeiss Microimaging GmbH, Berlin, Germany) was used to observe

the microstructure of the heat-treated glass–ceramics after etching in HF solution and coating with a thin carbon film. The TEM images and selected area electron diffraction (SAED) of the powdered glass–ceramic sample were obtained from an FEI (Model Tecnai G2 30ST, FEI Company, Hillsboro, OR) instrument. The FTIR reflectance spectra were traced using a FTIR spectrometer (Model 1615, Perkin Elmer), in the wave number range of 400–2000 cm^{-1} at resolution of ± 2 cm^{-1} after 16 scans. The optical absorption spectra were recorded on a Perkin Elmer UV-visible spectrophotometer (Model Lambda 20, Perkin-Elmer Corporation, Waltham, MA, USA) in the wavelength range of 400-1100 nm with an accuracy of ±1%. Capacitance and dielectric loss of the glasses and glass–ceramic nanocomposites were measured at room temperature using a Hioki LCR meter (Model 3532-50 Hitester, Hioki, Ueda, Nagano, Japan) at 1 MHz frequency after coating the surfaces with a conductive silver paint (here silver acts as an electrode) followed by drying at 140^0C for 1 h. The dielectric constants (ε_r) were calculated from the dimensions of the sample and the measured capacitance.

Results and discussion

Physical property

DTA study is a pre-requisite condition to determine heat-treatment condition for a glass system to convert it into a glass-ceramic with a desired crystalline phase. DTA trace for BiT45 glass exhibits an inflection in the temperature range of 400–470^0C followed by two moderate exothermic peaks at 598^0C (Tp_1) and 858^0C (Tp_2) (Fig. 1). DTA trace for BiT40 glass is also shown in Fig.1, which exhibits an inflection in the temperature range of 420–460^0C followed by two moderate exothermic peaks around 582^0C (Tp_1) and 848^0C (Tp_2)

(Fig. 1). Much difference in the glass transition temperatures (Tg) between the glass BiT45 (450^0C) and BiT40 (445^0C) are not observed. XRD studies were performed on the BiT45 glass samples heat treated at four different temperatures of 580^0C/1 h (BiT45C1) and 10 h (BiT45C2), 650^0C/2 h (BiT45C3), 800^0C/2 h (BiT45C4) and 930^0C/2 h (BiT45C5) to determine the crystal phases corresponding to the exothermic peaks in the DTA curve (Fig. 1). The sample designations are mentioned above within the parenthesis. Combining both XRD and DTA, it has been resolved that both the peaks are found to be due to the crystallization of BiT phase, as with increase in heat-treatment temperatures (800^0C and 930^0C), no additional phases are detected in XRD patterns (Fig. 7). Thermal expansion coefficient (CTE), glass transition temperature (T_g) and deformation temperature (T_d) measured for these glasses are presented in Table 1. The thermal properties of BiT10 glass (except T_s) could not be measured because it absorbs water at room temperature due to the presence of higher amount of alkali oxide (K_2O~30 mol%) in the glass. CTE was measured over the temperature range of 50-350^0C and it is evident from the data that with increasing BiT content in the glass the CTE is decreased. Komleva and Dmitrieva [28] have observed similar effects of lowering thermal expansion coefficient while studying the effect of replacement of silica in the sodium di-silicate glass by titanium. Such a behavior of thermal expansion co-efficient property indicates that titanium which apparently acts as a glass-former in four-fold coordination that facilitates the strengthening of the structure of the glasses [28]. From the Table 1, it is observed that with increase in BiT content in the glasses, the T_g, T_d and T_s values are also decreased gradually along with the CTE values. This decreasing trend in various thermal property values of the glasses are attributed to the presence of more amount of low melting Bi_2O_3 (melting temperature 824^0C) with

increasing BiT content. The values of T_g temperatures thus obtained for different glasses by dilatometer are similar to that found in DTA experiments. It is evident from Table 1 that there is a monotonic decrease of about 30^0C in T_g values of glasses with increasing BiT content. With increase in BiT content in the glasses, the glass network forming oxide SiO_2 reduces, hence, the viscosity of the glass and Tg is decreased. Previous researchers [25, 27] also noted that with decreasing content of network forming oxides, the glass transition temperatures are reduced. Due to decrease of network forming oxides in the glasses with the advent of BiT in the glasses, the viscosity and cross-linking is decreased, hence, deformation temperature (T_d) and softening temperature (T_s) is reduced. The density (d) of such glasses was also measured by adopting Archimedes principle. With increase in BiT content in the glasses, the density of glasses increases (Table 1). This increase in density with increasing BiT content in the glass is expected because less dense silica (2.20 $g.cm^{-3}$) and potassium oxides (2.35 $g.cm^{-3}$) are replaced with highly dense bismuth (8.90 $g.cm^{-3}$) and titanium oxides (4.23 $g.cm^{-3}$) in the glasses. These findings are in agreement with the observations of Gerth and Rüssel [27].

Optical property and third order susceptibility

The transmission spectra obtained for the glasses containing varying amount of BiT (x= 10, 20, 45 and 50) melted at 1150^0C are presented in Fig. 2. From the spectra, it is seen that with increasing BiT content in the glass, transmission of the glass in the wavelength range of 300-1100 nm decreases. The optical transmission cut-off wavelength ($\lambda_{cut\text{-}off}$) of these glasses shifts towards higher wavelengths with increase in BiT content, viz., 340 nm for BiT10 to 410 nm for BiT50. This change in cut-off wavelength observed is similar to the

findings of Shankar and Varma [26]. In fact, the cut-off wavelength obtained for this material is towards much lower wavelength than that of the reported by Shankar and Varma (420-490 nm). Further, systematic control experiment has been performed to study the effect of melting temperatures on the transmission property of the BiT45 glasses. This composition (BiT45) has been chosen because it contains maximum amount of BiT that can be produced by melt-quenching technique in air without any spontaneous crystallization. It is observed that with increasing melting temperatures of these glasses the transmission property in the visible wavelength range has been declined substantially (Fig. 3). Gerth and Rüssel [27] also observed that the color of the samples changes from yellow to brown depending on the composition and melting temperatures. They reported that samples possessing larger Bi_2O_3–concentrations are more intensely colored if melted at the same temperatures. The increase in melting temperature causes partial reduction of Bi_2O_3 to metallic bismuth (Bi^0). With increase in melting temperature, the redox equilibrium according to the Eq. (1) is shifted to the right side [29].

$$Bi_2O_3 \Leftrightarrow 2Bi^0 + \frac{3}{2}O_2 \qquad (1)$$

To verify this fact SAED pattern was obtained during TEM studies. Diffraction pattern shows the presence of rhombohedral Bi. The details of this study are provided in subsection (4) of FESEM and TEM Analysis. From the spectra shown in Fig. 3, it may be considered that the glass melting temperature 1050^0 C is optimum for this system in respect to the optical transmission point of view. It has been observed that if the glass is melted at 1050^0C, the glass produced will have the maximum transparency and the glass block can be made homogeneous and defect free (i.e. devoid of bubbles, un-melted batches etc.). The

darkening of the glass color with increasing melting temperature is also evident from the images taken (shown in Fig. 3 as inset) of as prepared glass samples.

The change in refractive index (n) with the wavelength of the glasses and with varying BiT content is shown in Fig. 4. RI was found to increase (from 1.5630 for BiT10 (not shown in the Fig. 4) to 1.9658 for BiT50, measured at 632.8 nm wavelength) with increasing BiT content in the glasses. This sharp increase in RI with increasing Bi_2O_3 and TiO_2 (i.e. BiT) content in the glasses occurs mainly because of the more dense structure of the glass obtained and also due to the incorporation of more polarisable as well as more ionic refraction of Bi and Ti ions present in the glass. To understand better the effect of composition on the RI, the empirical relation derived by Lorentz [30] and Lorenz [31] is used to estimate the molar refraction (R_M).

$$R_M = \frac{(n^2 - 1)}{(n^2 + 2)} \cdot \frac{M}{\rho} \qquad (2)$$

where ρ and M are the density and molecular weight of the glass respectively. Molar refraction R_M is related to the structure of glass and directly proportional to the optical polarizability [26] of the material, α_m, according to the following relationship:

$$\alpha_m = \frac{3}{4\pi N} \cdot R_M \qquad (3)$$

where N is the number of polarizable ions per mole, assumed to be equal to the Avogadro number. The values of R_M and α_m were estimated using Eqs. 2 and 3. The plot of polarizability, α_m against the composition of glasses is shown in Fig. 5. It shows that with increase in BiT content in the glass the optical polarizability of the glass increases almost linearly. These values are in agreement with findings of the previous researchers [22]. The

increase of polarizability is accompanied by an increase in molar refraction and hence by an increase in the RI. It results in the increase in polarizability of the glass. The linear and nonlinear optical properties of the glasses are determined by the bond polarizabilities [32]. This is due to the interaction of the propagating light with the electronic charge distribution in the glass structural units. The Bi^{3+} ion belongs to the group of ions with one lone-pair electron configuration [27]. This loan-pair electron exists at the apex of the pyramidal structure and easily polarizes on applying electric field and or in interaction with light. Researchers [32] showed with Raman spectroscopy study that Ti does not behave as simple network modifiers but rather behave as intermediates. They also established that the optical properties of multi-component oxide glasses are more influenced by the concentration of the transition metal cations rather than by the number of non-bridging oxygen. The nonlinear index in the present system is controlled by the nonlinear bond polarizability of the Ti-O bonds. It has also been reported that ions with an empty or unfilled d shell (e.g. Ti) contribute greatly to the linear and nonlinear polarizabilities [32].

The Abbe number (υ_d) obtained for different glasses with varying BiT content also demonstrates that with increasing BiT content the υ_d of the glass is decreases. Abbe numbers were calculated from a well-known empirical relation using RI of light at different wavelengths, the values thus obtained are plotted against RI (n_d, 587.6 nm) is shown in Fig. 6. It is evident that all these glasses belong to the family of high index and high dispersion comparable to the high lead bearing glasses.

An attempt was made to estimate the third order susceptibility, χ^3, using an indirect method. According to Boling's [33] semi empirical equation, χ^3 of a materials is strongly

dependent on both the nonlinear refractive index (n_2) and linear refractive index (n). χ^3 is expressed by the following relation, according to Vogel et al. [32]

$$\chi^3 = \frac{n}{12\pi} \cdot n_2 = \frac{17}{3\pi} \cdot \frac{(n-1)(n^2+2)^2}{\upsilon_d [1.52 + (n^2+2)(n+1)\frac{\upsilon_d}{6n}]^{0.5}} \qquad (4)$$

where n is refractive index of glass at 587.6 nm and n_2 is non-linear refractive index estimated from an empirical relation derived by Vogel et al. [32]. The χ^3 is shown in Fig 5. The susceptibility values estimated from the above equation (4) shows that with increase in BiT content in the glass, the χ^3 values increases steadily. The values thus estimated were found to be in order with the values reported for oxide glasses by previous researchers [34,35,36].

XRD analysis

XRD studies were performed on the BiT45 glass samples heat treated at four different temperatures of 580^0C/1 h (BiT45C1) and 10 h (BiT45C2), 650^0C/2 h (BiT45C3), 800^0C/2 h (BiT45C4) and 930^0C/2 h (BiT45C5) to determine the crystal phases evolved after ceramization. Heating and cooling rate of 2^0C/min for BiT45C1 samples and for other samples 1^0C/min was maintained. BiT45 glass composition was selected for heat-treatment experiments because it contains maximum amount of BiT i.e. x=45 and it possesses highest optical transmission among all the glasses studied here.

XRD patterns of the heat-treated glass-ceramic samples BiT45C1, BiT45C2, BiT45C3, BiT45C4 and BiT45C5 has been shown in Fig. 7 and marked as a, b, c, d and e respectively. All these samples have become completely opaque after heat-treatment. The

major crystalline phase identified in all the glass-ceramics was BiT ($Bi_4Ti_3O_{12}$). The diffraction pattern has been compared with JCPDS file card no. 35-0795 and marked with B in the XRD patterns. It has been determined that with increase in heat-treatment time there was no signature of additional peaks developed therein. XRD peaks are broader for the samples BiT45C1, BiT45C2 and BiT45C3 whereas, sharp peaks are detected for the samples BiT45C4 and BiT45C5 which are heat-treated at comparatively higher temperatures. In XRD pattern broader peaks are generated due to smaller crystallite sizes and sharp peaks are due to the formation of comparatively bigger crystallites. To establish this fact, from the full width at half maximum (FWHM) of the intense diffraction peak of $Bi_4Ti_3O_{12}$, the average crystallite size (diameter, t) is calculated by using Scherrer's formula [37].

$$t = \frac{0.9\lambda}{\beta Cos\theta} \qquad (5)$$

where λ is the wavelength of X-ray radiation (CuKα = 1.5406 Å) and β is the full-width at half-maximum (FWHM) of the peak at 2θ. The average crystallite size increases with heat-treatment duration marginally and was found to vary in the range of 2–3 nm for samples BiT45C1 (580^0C/1 h), BiT45C2 (580^0C/10 h) and BiT45C3 (650^0C/2 h). However, the crystallite size was found to increase significantly with increase in heat-treatment temperature up to 30 and 39 nm for the samples BiT45C4 (800^0C/2 h) and BiT45C5 (930^0C/2 h) respectively. At higher temperatures diffusion of ions in the glasses is increased, hence the crystals growth rate is accelerated and bigger size crystals result in after heat-treatment.

FESEM and TEM analyses

Field emission scanning electron microscopic (FESEM) and transmission electron microscopic (TEM) observations have been carried out to investigate nucleation and crystallization phenomena. FESEM micrographs of BiT45 glass-ceramics heat-treated at 580^0C for 1 h (BiT45C1) has been shown in Fig. 8(a). The micrograph shows that polycrystalline granules of uniform size are homogeneously dispersed in the glass matrix. XRD analysis reveals that crystallite sizes are in the range of 2-3 nm only, whereas, FESEM micrograph shows that spherical grains of sizes 70-80 nm are formed. From this fact, it may be ascertained that the glass-ceramics developed in the present investigation are polycrystalline material. These polycrystals are made up of a large number of tiny crystallites held together by thin layers of amorphous solid, hence the size of the polycrystals are bigger than crystallites. Development of polycrystals in a base glass generally takes place in two stages: formation of nuclei and subsequently their growth into crystals in the phase separated part rich in crystal forming components. A nucleus is an entity that already belongs to the new phase but is in unstable equilibrium with respect to the supersaturated parent phase. The thermodynamic driving force of the glass-crystal transition is the chemical potential or free energy between the separated phase and the crystal[38]. In the present case, heterogeneous nucleation was catalyzed using refractory TiO_2 (melting point = 1850^0C) particles. Two distinct phases were evolved during nucleation, one is TiO_2 and Bi_2O_3 rich phase and other one is SiO_2 and K_2O rich phase. During heat-treatment, TiO_2 and Bi_2O_3 rich phase was grown to form $Bi_4Ti_3O_{12}$ polycrystals out of the $Bi_4Ti_3O_{12}$ crystallites. In the case of BiT45C2, where a heat-treatment was employed for an extended period of 10 h, the average crystalline particle size was observed increased in size

(80-90) nm (Fig. 8 b). The glass phase was decreased over the increase in heat-treatment time, which establishes the fact that more glass is converted into crystal during heat-treatment. Interestingly, it has also been observed that with increase in heat-treatment time (BiT45C2) the granular polycrystals are merged with one another making nano-rods of diameter 85-90 nm (Fig. 8 b). Researchers worked on this system, reported sheaf-shaped, rod like [27], platelets [39] crystals of dimension in the micrometer range, crystals of platy morphology [22] with the dimension in the nanometer range has also been reported. However, for this system formation of glass-ceramics with nano-rod morphology are not reported previously. Critical examination of the rods formed and the similarity between the dimension of the crystal grains and the rod diameter reveals that grains are connected side by side epitaxially which leads to the formation of this kind of nano-rod morphology. These rods are also observed to cross-link with each other. Hence, this is a new and interesting findings and its influence on the properties of the materials needs to be studied in details.

EDS analysis of the crystals show Bi peaks of highest intensity (Fig. 8c), followed by O. Si and K peaks of almost equal intensity are also visible. However, weak Ti peaks are observed. From such observations, it should be clear that the crystals are Bi rich.

Further, TEM observation was carried out to examine the crystallization behaviour of the heat-treated glass-ceramics. The bright field TEM image of BiT45C2 glass-ceramics along with respective SAED pattern has been shown in Fig 9. The nano-crystalline nature of the material is confirmed from the diffused hallow of SAED pattern obtained from the glass-ceramic. Further, indexing of the SAED pattern (shown as inset in Fig. 9) reveals that black particles of diameter 8-12 nm shown in image are due to the formation of Bi^0 metallic particles. These metallic particles are formed due to the reduction reaction (Eq. 1, discussed

earlier) took place at melting temperature ≥ 1050 ^{0}C. The (hkl) planes obtained from the pattern are matching with the rhombohedral Bi^0 (JCPDS file no. 44-1246) are indicated in the image. The TEM image also reveals the presence of nano crystals of BiT (2-3 nm black spots) in the glass-ceramics. TEM observation of crystallite sizes of the BiT correlates well with that determined using Scherrer's equation. However, a white glow is observed in the SAED pattern that supports the formation of nano crystallites of BiT in the glass-ceramics.

FTIR reflectance spectroscopy

The FTIR reflectance spectra of the as-prepared samples, BiT50, BiT40 and BiT20 in the wavenumber range of 400–2000 cm^{-1} are shown in Fig. 10. The Si-O-Si band positions and intensity of the reflectance at the band has been plotted and shown in the inset of Fig. 10. Si-O-Si bands are evident from the reflectance spectra at 900-1000 cm^{-1}. The analysis of the results also reveals that with increase in BiT content in the glass, this Si-O-Si band intensity is reduced. This is due to the fact that amount of SiO_2 in the glass decreases with increase in BiT. It has also been noted that with increase in BiT content, the intensity of reflectance increases at around 500 cm^{-1}. Ardelean [40] et. al reported the presence of absorption peaks due to the stretching vibrations of Bi-O bonds in strongly distorted BiO_6 octahedral units at 490 cm^{-1} in the FTIR absorption spectra. This observation clearly indicates that, this phenomenon may be attributed to the fact that with increase in BiT content, the extent of Bi_2O_3 in the glass increases, which results in increase in the intensity of reflectance at around 500 cm^{-1}. The isosbestic point was observed at 715 cm^{-1}, which indicates that there is equilibrium between the silicate and bismuth containing species.

Dielectric property

Glass and glass–ceramics have certain advantages as dielectric materials because of their high dielectric strength. However, the disadvantages of glass are a low permittivity (ε_r = 4–15) and a low thermal conductivity [41]. In the present investigation, the as-prepared BiT glass has exhibited a relatively higher value of dielectric constant (ε_r) (14-22) than that of the common glasses such as vitreous silica (3.8), soda-lime silicate (7.2) or borosilicate glasses (4.1–4.9) [42] and similar to that of the Li_2O–Ta_2O_5–SiO_2–Al_2O_3 glasses [43] studied recently in our group. The change in dielectric constant with varying concentration of BiT in the glasses is depicted in Fig. 11. It is observed that with increase in BiT content in the glasses the dielectric constant increases. A significant increase of ε_r value (from 21 to 39) was observed for the corresponding glass-ceramics heat-treated at 580^0C for 1 h (BiT45C1) and 10 h (BiT45C2). However, there is minor increase (~4) in ε_r value was observed when BiT45 glass was heat-treated at 580^0C for 10 h (38.5) compared to 1 h (34.5). This small increase in ε_r value reconfirms that with increase in heat-treatment time at an elevated temperature increases the quantity of ferroelectric $Bi_4Ti_3O_{12}$ crystals in the glass-ceramics. Hence, this increase in ε_r values with increase in heat-treatment time at a particular crystallization temperature is justified as the crystals developed after heat-treatment is ferroelectric ($Bi_4Ti_3O_{12}$). Ferroelectric non-centrosymmetric $Bi_4Ti_3O_{12}$ crystals formed after heat-treatment of glass, which results in the increase in the dielectric constant. This increase in ε_r value can be anticipated because polycrystalline $Bi_4Ti_3O_{12}$ ceramics has higher ε_r (~150) compared to the base glass (14-22) [44]. Hence, when the glass is subjected to a heat-treatment for ceramization and a fair amount of glass is converted in to glass-ceramics containing ferroelectric $Bi_4Ti_3O_{12}$ phase, the ε_r value is likely to increase.

This is due to the very high ionic refraction (Bi-30.5 and Ti-19.0) and polarizability [45] (Bi-1.31 and Ti-0.46) of Bi^{3+} and Ti^{4+} ions present in the material. The increase in ε_r with increasing BiT content is attributed mainly to the increase in interfacial polarization caused by the presence of ferroelectric non-centrosymetric BiT crystallites in the glassy matrix.

The dielectric loss (D) of the glasses as well as glass-ceramics is measured and summarized in Fig. 11. The dielectric loss data shows that with increasing BiT content in the glasses the loss value is decreased gradually. The D values obtained for the glasses and glass-ceramics are in the very low range of 0.0441- 0.00374 and 0.01404- 0.01994 respectively. This decrease in D values is attributed to the reducing concentration of alkali ion (k^+) charge carriers with increase in BiT (Bi_2O_3 and TiO_2) content in the glass in expense of SiO_2 and K_2O. Electrical property of a glass is primarily controlled by the connectivity of the continuous glassy phase and this glass phase is reduced and crystalline phases are increased after heat-treatment. As BiT45C1 contains less crystals compared to BiT45C2, its dielectric loss is more compared to BiT45C2. Murugan et. al [15] have also observed that the dielectric loss (D) decreases with increasing ferroelectric phases in the glass-ceramics and they also reported that D value is less for glasses compared to the polycrystalline ceramics in the same system. Achieving a reduction of the low D value and enhancement of ε_r in glass-ceramics has been an important consideration for device applications.

Conclusions

The influence of $Bi_4Ti_3O_{12}$ (BiT) content in the K_2O-SiO_2-Bi_2O_3-TiO_2 glass system on the various properties has been demonstrated. Properties and microstructural changes occurred

due to formation of glass-ceramics are also discussed. DTA, dilatometer, XRD, FESEM, TEM, and FTIRRS were used for their characterization. Optical and third order susceptibility of the glass samples have been evaluated using prism coupler and UV-Vis spectrophotometer. The important conclusions are summarized as:

- Studies on effect of melting temperatures on the transparency of the glasses reveal that for the K_2O-SiO_2-Bi_2O_3-TiO_2 (KSBT) system melting temperature of 1050^0C gives optimum transparency. The darkening of the glass color with increasing melting temperature is due to a partial reduction of Bi^{3+} ion to metallic bismuth Bi^0.
- With increase in BiT content in the glass the density increases whereas coefficient of thermal expansion (α), glass transition temperature (T_g), deformation temperature (T_d) and softening temperature (T_s) of the glasses decrease monotonically.
- Systematic increase in refractive index and third order susceptibility with increase in BiT content of the glass has been observed due to very high ionic refraction and polarizability of Bi and Ti ions.
- XRD studies of glass-ceramics confirm the formation and growth of ferroelectric $Bi_4Ti_3O_{12}$ crystals.
- Microstructural studies show that granular polycrystals of 70-90 nm and nano rods of average diameter 85-90 nm were developed in the samples heat-treated at $580\ ^0$C for 1 h and 10 h respectively. This is the first report for the formation of the crystals with nano-rod morphology in the KSBT glass system.
- A systematic increase in dielectric constant (ε_r) values (14-22) has been observed with increase in BiT content in the glass which is considerably higher than that of the common glasses. A steep increase in ε_r value of heat-treated glass-ceramic (39)

have been noticed compared to its precursor glass due to the formation of ferroelectric noncentrosymetric $Bi_4Ti_3O_{12}$ crystals having high dielectric constant. The dielectric loss values (0.01404-0.0441) are considerably less which is important with respect to their device application point of view.

Acknowledgements

The authors thank Director of the Institute for his keen interest and kind permission to publish this paper. Electron Microscope and X-Ray Divisions of the Institute are also thankfully acknowledged.

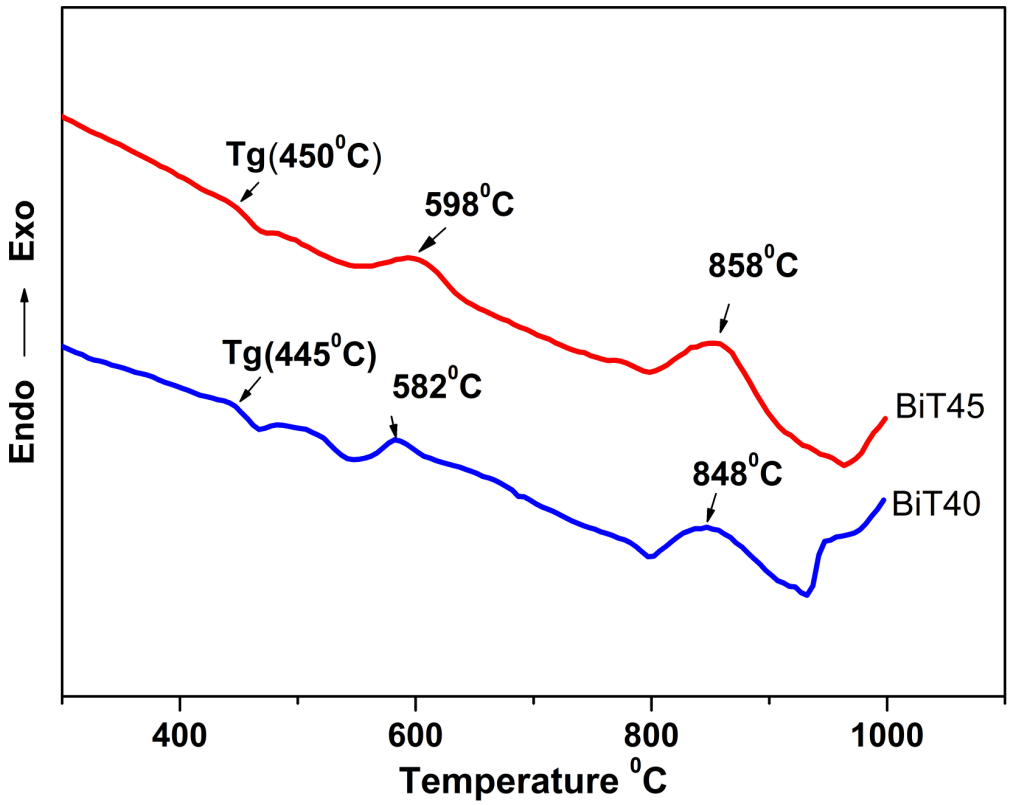

Fig. 1. DTA thermogram of BiT40 and BiT45 glass powders.

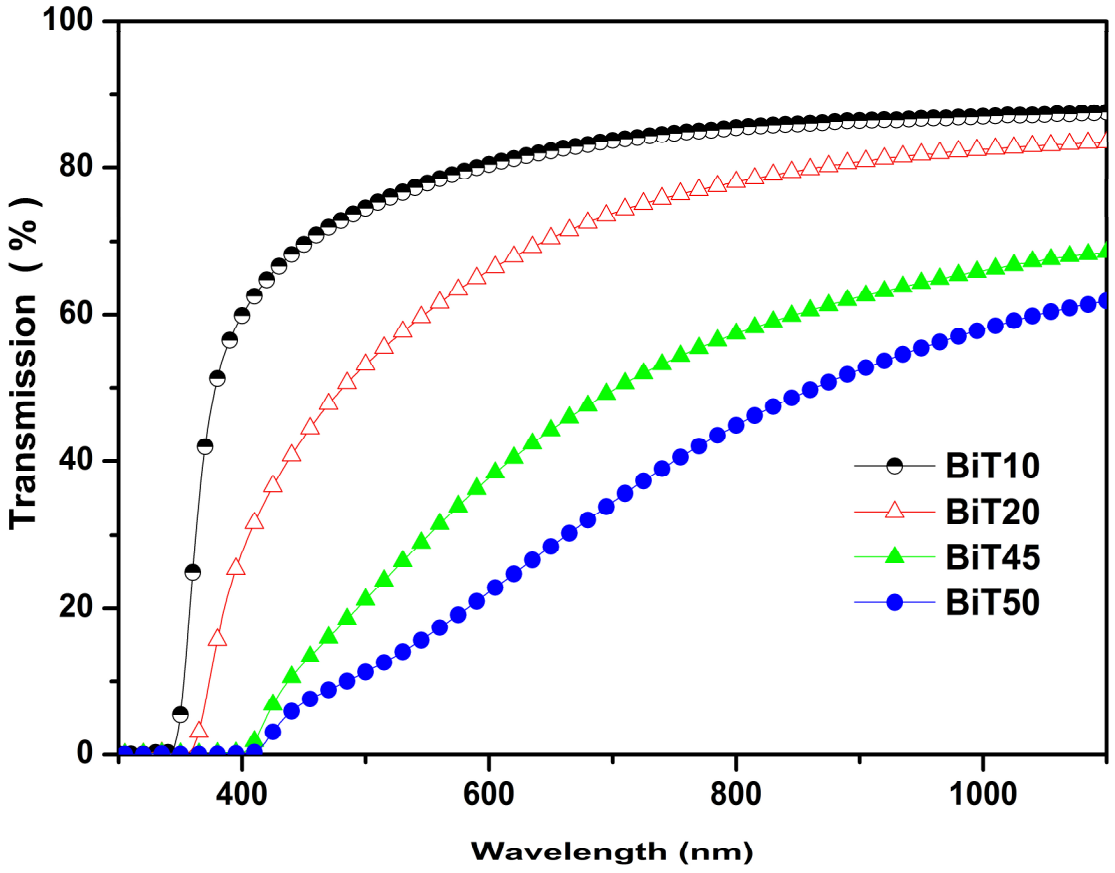

Fig. 2. (Color online) Transmission spectra of BiT10, BiT20, BiT45 and BiT50 glasses melted at 1150^0 C (Thickness of glass = 2 mm).

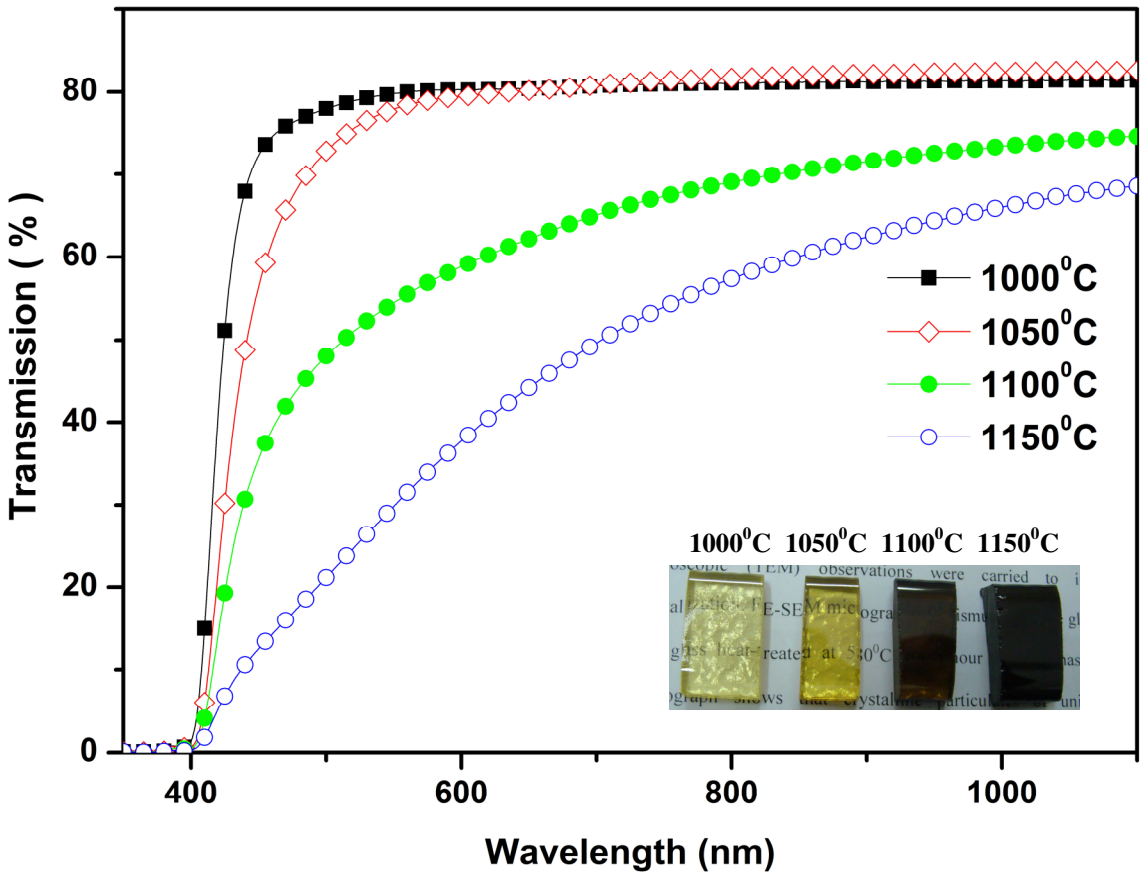

Fig. 3. (Color online) Transmission spectra of BiT45 glasses melted at 1000, 1050, 1100 and 1150^{0}C (Thickness of glass = 2 mm). Inset is the photograph of the glasses showing their visual transparency as laid on writing.

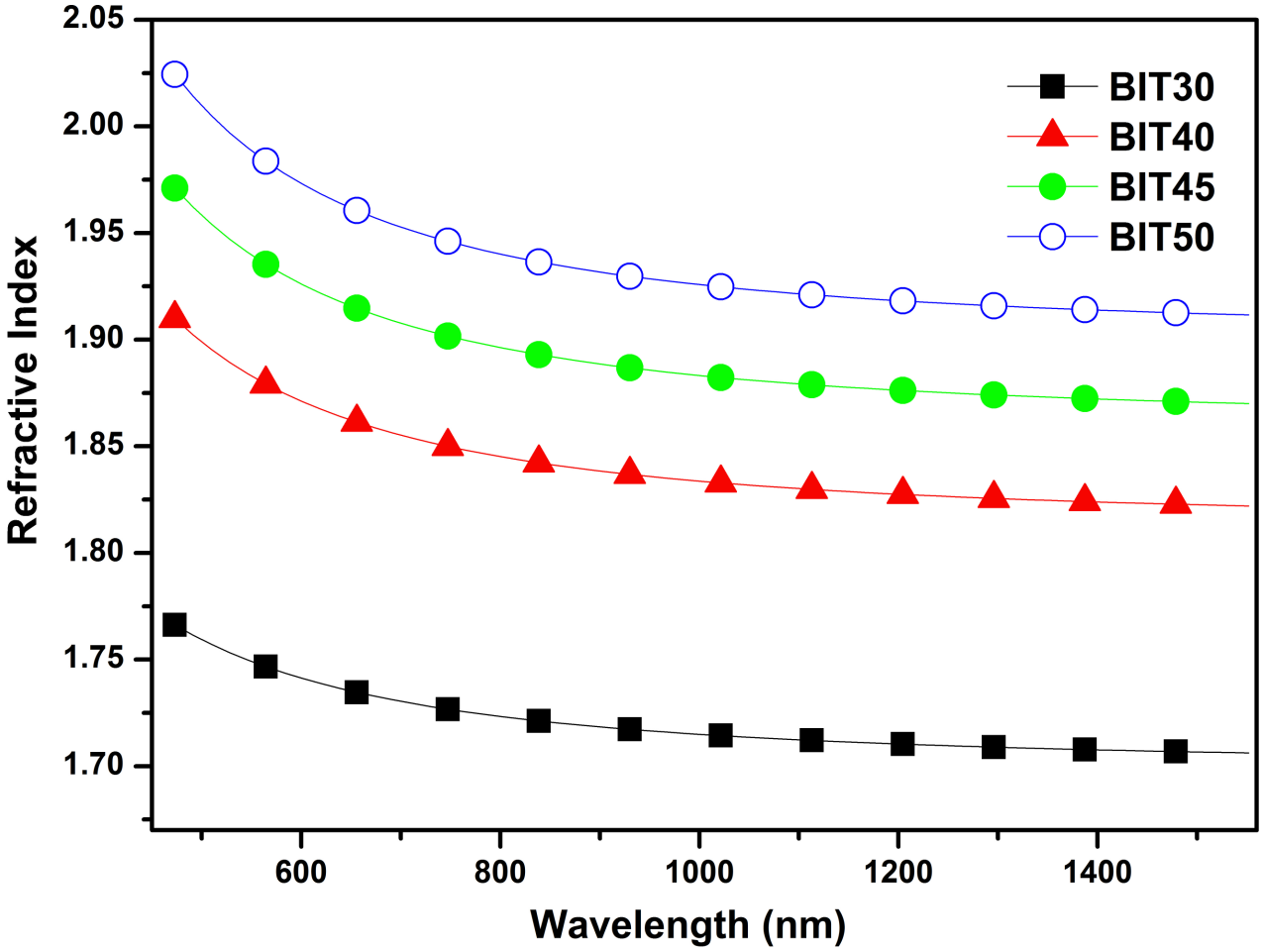

Fig.4. (Color online) Variation of refractive index as a function of wavelength of BiT30, BiT40, BiT45 and BiT50 glasses.

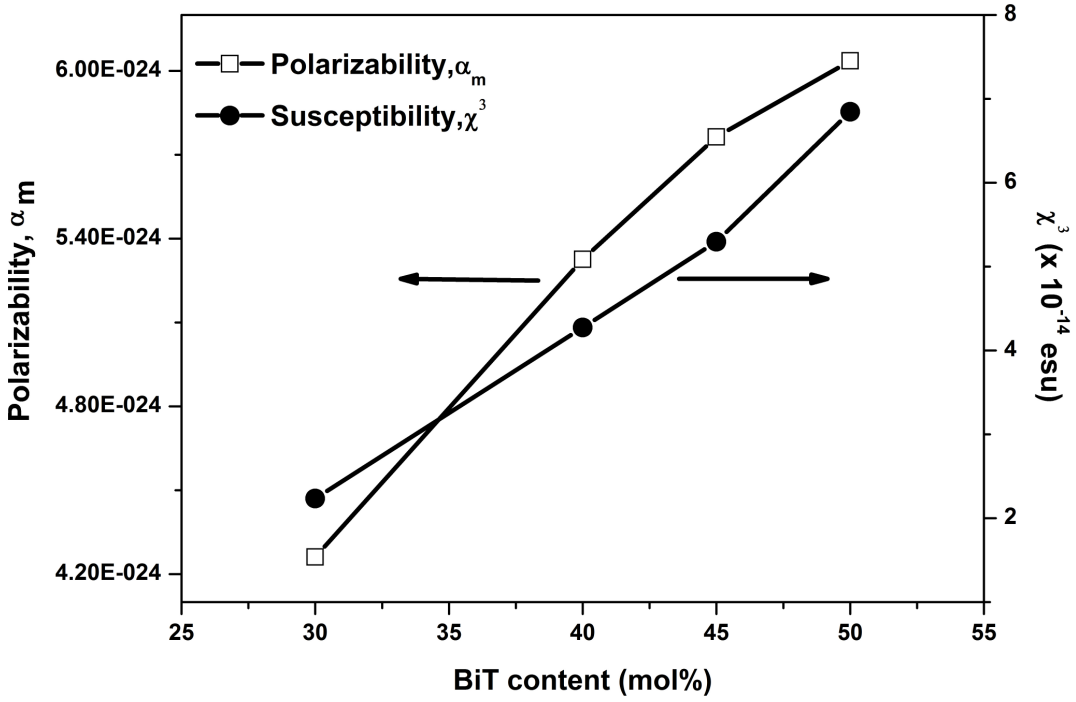

Fig. 5. Polarizability (α_m) and third order susceptibility (χ^3) as a function of BiT content in glasses.

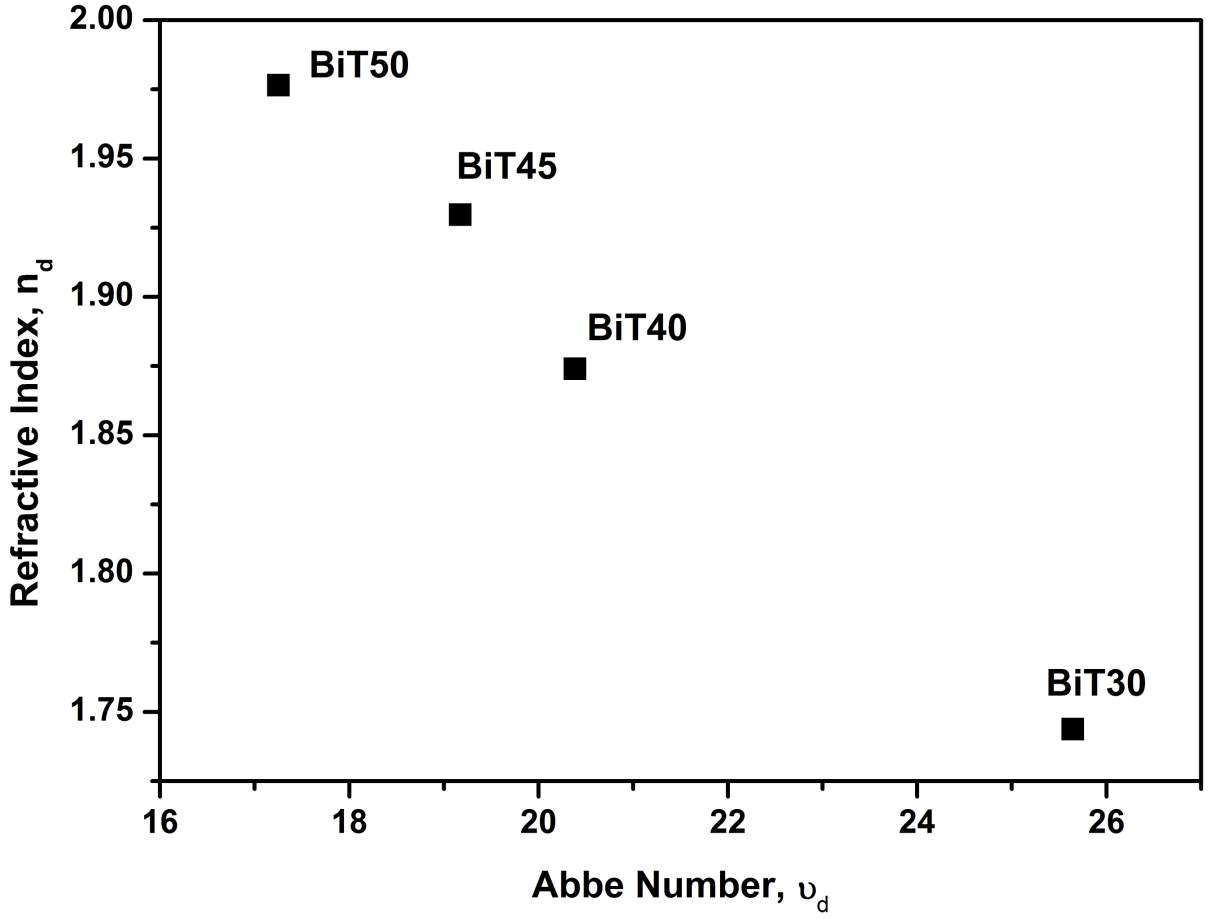

Fig. 6. Location of BiT30, BiT40, BiT45 and BiT50 glasses in the Abbe diagram (n_d vs. υ_d).

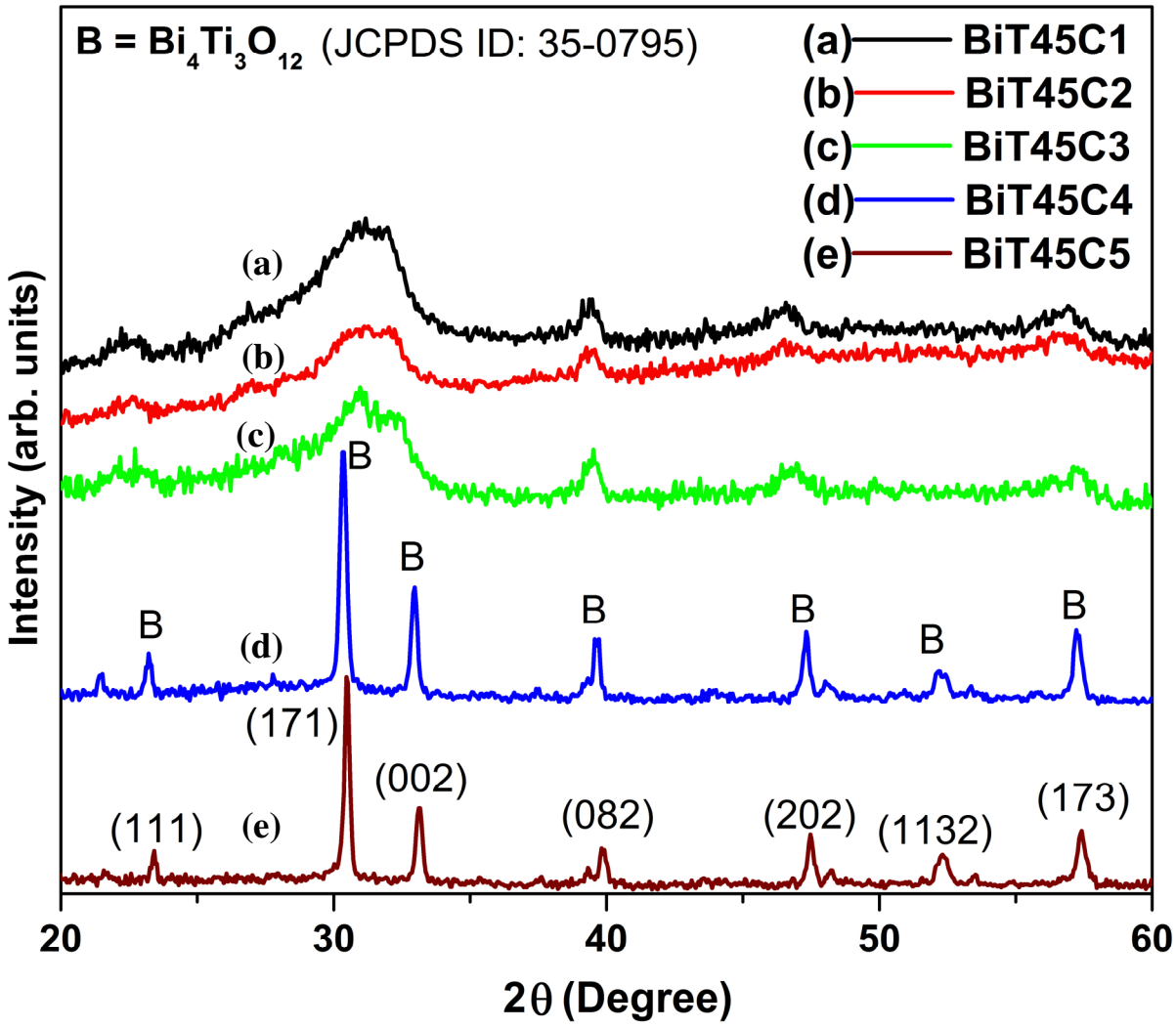

Fig. 7. (Color online) XRD patterns of bismuth titanate glass-ceramics derived from BiT45 glass heat-treated at (a) 580^{0}C for 1 h (BiT45C1), (b) 580^{0}C for 10 h (BiT45C2), (c) 650^{0}C for 2 h (BiT45C3), (d) 800^{0}C for 2 h and (BiT45C4) (e) 930^{0}C for 2 h (BiT45C5).

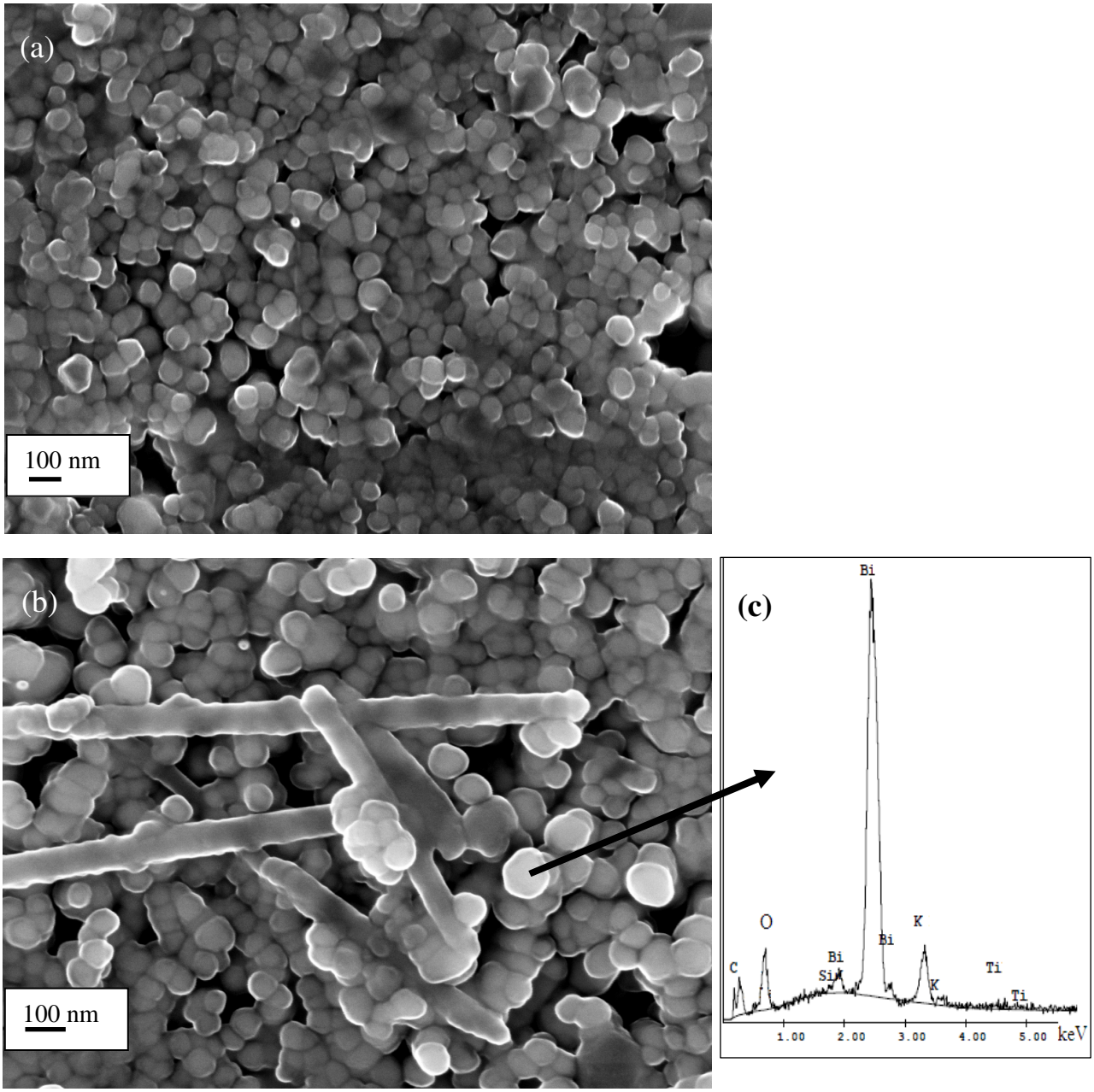

Fig. 8. Secondary electron FESEM images disclose the microstructures of the glass-ceramics derived from BiT45 glass heat-treated at (a) 580^0C for 1 h (BiT45C1), (b) 10 h (BiT45C2) and (c) EDS spectrum of spherical grains, black arrow indicates the grain on which the spectrum was taken.

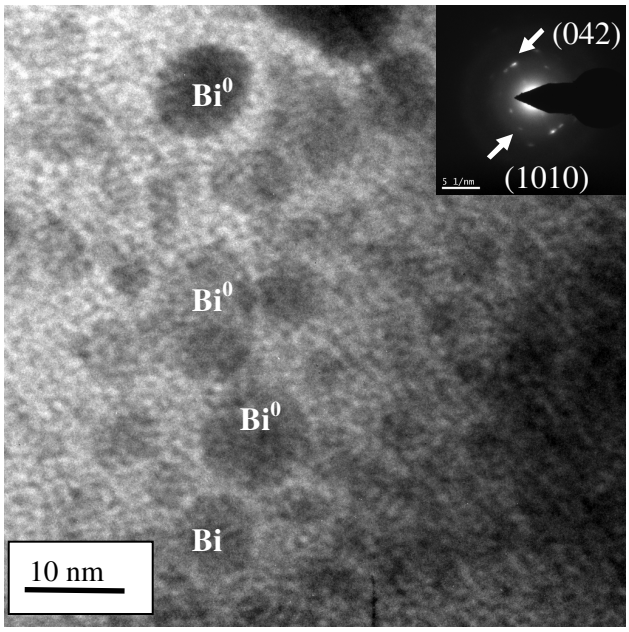

Fig. 9. TEM image of the BiT45C2 glass-ceramics heat-treated at 580^0C for 10 h (inset shows the SAED pattern).

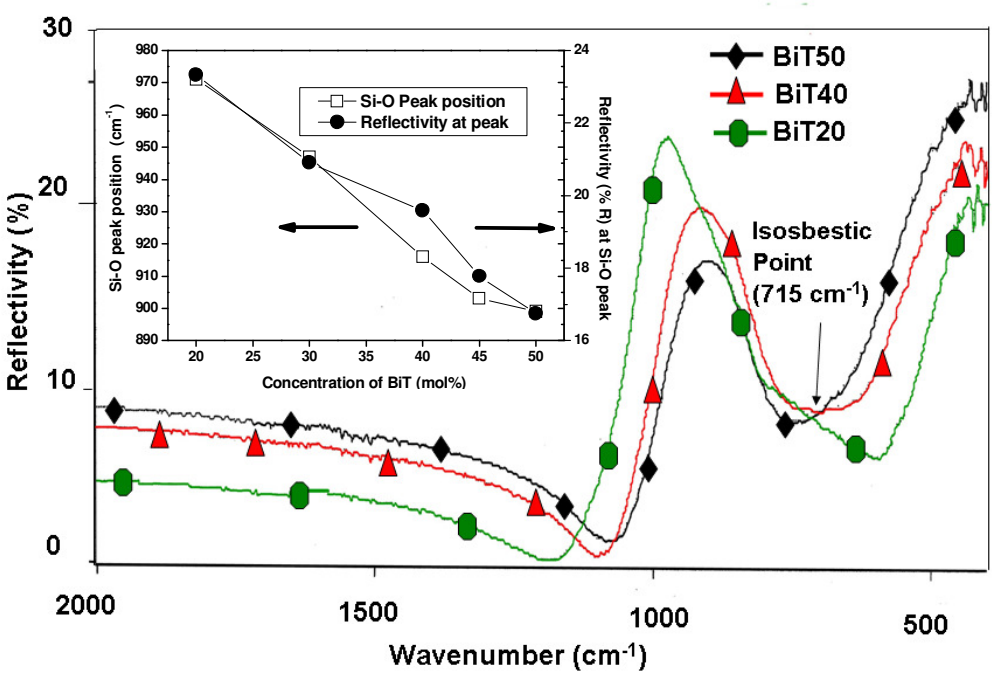

Fig. 10. (Color online) Fourier transformed infrared reflectance spectra of samples BiT20, BiT40 and BiT50. Inset shows variation of Si-O band positions and its reflectivity as a function of BiT content in the glasses.

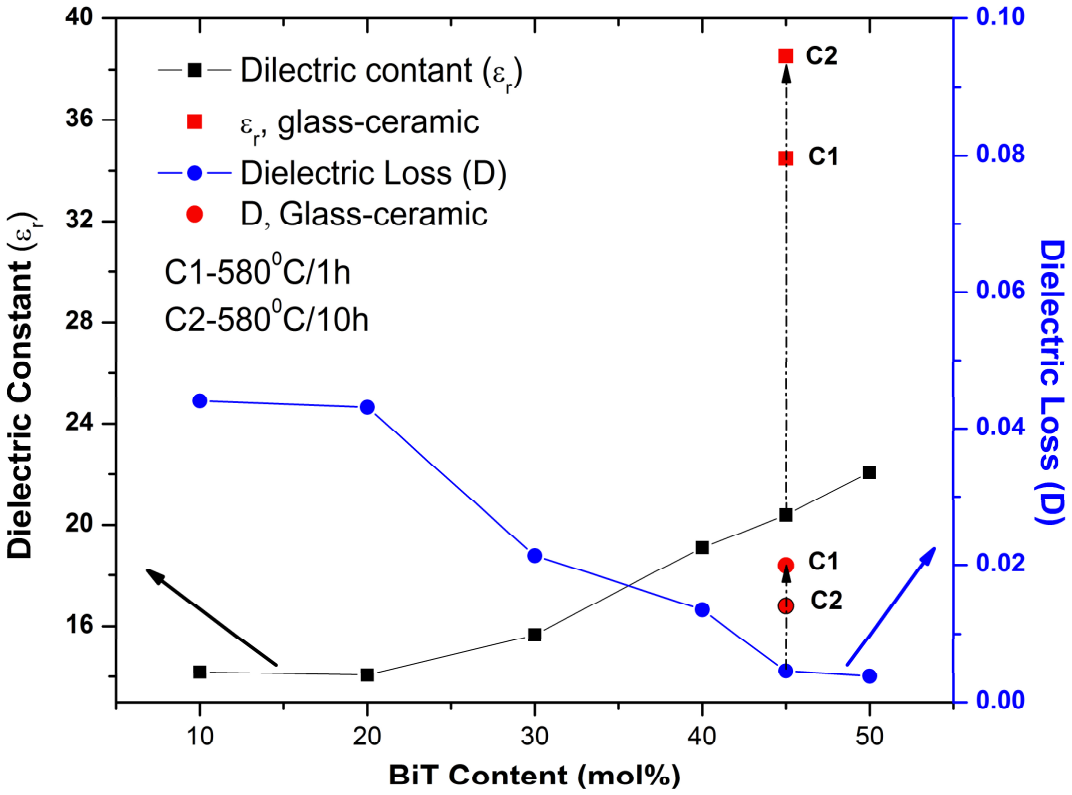

Fig. 11. (Color online) Dielectric constant (ε_r) and dielectric loss (D) of the glasses BiT10, BiT20, BiT30, BiT40, BiT45, BiT50 and glass-ceramics BiT45C1 and BiT45C2 as a function of BiT content.

References

1. Borrelli NF, Herczog A, Maurer RD (1965) Electro-optic effect of ferroelectric microcrystals in a glass matrix. Appl Phys Lett 7: 117-118

2. Borrelli NF (1967) Electro-optic effect in transparent niobate glass-ceramic system. J Appl Phy 38 (11): 4243-4247

3. Jain H (2004) Transparent ferroelectric glass-ceramic. Ferroelectrics 306 :111–127

4. Corker DL, Zhang Q, Whatmore RW , Perrin C (2002) PZT composite ferroelectric thick films. J Eur Ceram Soc 22:383-390

5. Villegas M, Jardiel, T Caballero AC (2009) Effect of ZnO on the microstructure and electrical properties of WO_3–$Bi_4Ti_3O_{12}$ ceramics. J Eur Ceram Soc 29: 737–742

6. Hosoka M, Nogi K, Naito M , Yokoyama Y (2007) Nanoparticle Technology Handbook. Elsevier, Amsterdam

7. Aurivillius B (1949) Mixed bismuth oxides with layer lattices ii: structure of $Bi_4Ti_3O_{12}$. Ark Kemi 1: 499–512

8. Newnham RE, Wolfe RW, Dorrian JF (1971) Structural basis of ferroelectricity in the bismuth titanate family. Mat Res Bull 6 :1029-1040

9. Villegas M, Jardiel T, Caballero AC, Fernández JF (2004) Electrical properties of bismuth titanate based ceramics with secondary phases. J Electroceram 13: 543–548

10. Kojima S, Hushur A, Jiang F, Hamazaki S, Takashige M, Jang MS, Shimada S (2001) Crystallization of amorphous bismuth titanate. J Non-cryst Solids 293-295: 250-254

11. Fouskova A, Cross LE (1970) Dielectric properties of bismuth titanate. J Appl Phys 41: 2834-2838

12. Villegas M, Caballero AC, Moure C, Dur'an P, Fern´andez JF (1999) Factors Affecting the electrical conductivity of donor-doped $Bi_4Ti_3O_{12}$ piezoelectric ceramics. J Am Ceram Soc 82(9): 2411-2416

13. Villegas M, Caballero AC, Fern´andez JF, (2002) Modulation of electrical conductivity through microstructural control in $Bi_4Ti_3O_{12}$-based piezoelectric ceramics. Ferroelectrics 267(1) :165-173

14. Hirayama C, Subbarao EC (1962) Glass Dielectric properties of bismuth borate glasses. Phys Chem 3: 111-115

15. Murugan GS, Subbanna GN, Varma KBR (1999) Nanocrystallization of Ferroelectric bismuth tungstate in lithium borate glass matrix. J Mat Sci Lett 18: 1687–1690

16. Vernacotala DE, Chatlani S, Shelby JE (2000) Applications of Ferroelectrics 2000 Proceedings of the 12th IEEE International Symposium on Applications of Ferroelectric. Honolulu Hawaii, U.S.A

17. Borrelli NF, Layton MM (1968) Symposium on Applications of Ferroelectricity Electrooptic properties of transparent ferroelectric glass-ceramic systems. Catholic University of America, Washington D. C.

18. Bell AJ (2008) Ferroelectrics: the role of ceramic science and engineering. J Eur Ceram Soc 28: 1307–1317

19. Pengpat K, Holland D (2004) Ferroelectric glass-ceramics from the $PbO–GeO_2–Nb_2O_5$ system. J Eur Ceram Soc 24: 2951–2958

20. Graca MPF, Ferreira da Silva MG, Valente MA (2007) Structural and electrical properties of $SiO_2–Li_2O–Nb_2O_5$ glass and glass-ceramics obtained by thermoelectric treatments. J Mater Sci 42:2543–2550

21. Graca MPF, Valente MA, Ferreira da Silva MG (2006) The electric behavior of a lithium-niobate-phosphate glass and glass-ceramics. J Mater Sci 41:1137–1144

22. Shankar MV, Varma KBR (1998) Crystallization of ferroelectric bismuth vanadate in Bi_2O_3–V_2O_5–SrB_4O_7 glasses. J Non-Cryst Solids 226:145–154

23. Pengpat K, Holland D (2003) Glass-ceramics containing ferroelectric bismuth germanate (Bi_2GeO_5). J Eur Ceram Soc 23: 1599–1607

24. Ruiz-Valdés JJ, Gorokhovsky AV, Escalante-García JI, Mendoza-Suárez G (2004) Glass–ceramic materials with regulated dielectric properties based on the system BaO–PbO–TiO_2–B_2O_3–Al_2O_3. J Eur Ceram Soc 24: 1505–1508

25. Bengisu M, Brow RK, Wittenauer A (2008) Glasses and glass-ceramics in the SrO–TiO_2–Al_2O_3–SiO_2–B_2O_3 system and the effect of P_2O_5 additions. J Mater Sci 43:3531–3538

26. Shankar MV, Varma KBR (1998) Crystallization, dielectric and optical studies on strontium tetraborate glasses containing bismuth titanate. Mater Res Bull 33(12): 1769–1782

27. Gerth K, Rüssel C (1997) Crystallization of $Bi_4Ti_3O_{12}$ from glasses in the system Bi_2O_3/TiO_2/B_2O_3. J Non-cryst Solids 221: 10-17

28. Komleva GP, Dmitrieva VI (1969) Thermal expansion coefficient of titanium-containing glasses and enamels. Glass and Ceramics 26(11): 657- 669

29. Russel C, Freude E (1989) Voltametric Studies of the redox behavior of various multivalent ions in soda-lime-silica glass melts. Phys Chem Glass 30: 62-67

30. Lorentz HA (1880) Ueber die beziehung zwischen der fortpflanzungsgeschwindigkeit des lichtes und der koreperdichte. Ann Phys 9: 641-665

31. Lorenz R (1880) Ueber die refractionsconstante. Ann Phys 11: 70-103

32. Vogel EM, Weber MJ, Krol DM (1991) Nonlinear optical phenomena in glass. Phys Chem Glass 32: 231-254

33. Boling NL, Glass AJ, Owyoung A (1978) Empirical relationships for predicting nonlinear refractive index changes in optical solids. IEEE J Quantum Electron 14: 601-608

34. Adair R, Chase LL, Payne SA (1987) Non-linear refractive index measurements of glasses using three-wave frequency mixing. J Opt Soc Am B 4(6): 875-881

35. Hall DW, Newhouse MA, Borreli NF, Dumbaugh WH, Weidman DL (1989) Nonlinear optical suceptibilities of high index glasses. Appl Phys Lett 54: 1293-1295

36. Thamozaeu I, Etehepare J, Grillon G, Migus A (1985) Electronic nonlinear optical susceptibilities of silicate glasses. Optic Lett 10: 223-225

37. Cullity BD (1978) Elements of X-Ray Diffraction, 2nd edition. Addison-Wesley Publishing Co., London

38 Holand W and Beal G (2002) Glass-ceramic Technology. The American Ceramic Society, Ohio

39. Jardiel T, Rubia MA de la, Peiteado M (2008) Control of functional microstructure in WO_3-doped $Bi_4Ti_3O_{12}$ ceramics. J Am Ceram Soc 91(4): 1083–1087

40. Ardelean I, Cora S, Rusu D (2008) EPR and FT-IR spectroscopic studies of Bi_2O_3–B_2O_3– CuO glasses. Physica B 403: 3682–3685

41. Moulson AJ, Herbert JM (1990) Electroceramics Material, Properties Applications. Chapman & Hall, London

42. Blech IA (1986) In: Fink DG, Christiansen D (ed) Properties of Materials Electronics Engineering Handbook, 2nd edition. McGraw-Hill, New York

43. Tarafder A, Annapurna K, Chaliha RS, Tiwari VS, Gupta PK, Karmakar B (2009) Processing and properties of Eu^{3+}:$LiTaO_3$ transparent glass–ceramic nanocomposites. J Am Ceram Soc 92: 1934-1939

44. Watanabe H, Kimura T, Yamaguch T (1991) Sintering of platelike bismuth titanate powder compacts with preferred orientation. J Am Cer Soc 74:139-147

45. Volf MB (1984) Chemical Approach to Glass. Elsevier, Amsterdam

Figure Captions

Fig. 1. DTA thermogram of BiT40 and BiT45 glass powders.

Fig. 2. (Color online) Transmission spectra of BiT10, BiT20, BiT45 and BiT50 glasses melted at 1150^0 C (Thickness of glass = 2 mm).

Fig. 3. (Color online) Transmission spectra of BiT45 glasses melted at 1000, 1050, 1100 and 1150^0C (Thickness of glass = 2 mm). Inset is the photograph of the glasses showing their visual transparency as laid on writing.

Fig. 4. (Color online) Variation of refractive index as a function of wavelength of BiT30, BiT40, BiT45 and BiT50 glasses.

Fig. 5. Polarizability (α_m) and third order susceptibility (χ^3) as a function of BiT content in glasses.

Fig. 6. Location of BiT30, BiT40, BiT45 and BiT50 glasses in the Abbe diagram (n_d vs. υ_d).

Fig. 7. (Color online) XRD patterns of bismuth titanate glass-ceramics derived from BiT45 glass heat-treated at (a) 580^0C for 1 h (BiT45C1), (b) 580^0C for 10 h (BiT45C2), (c) 650^0C for 2 h (BiT45C3), (d) 800^0C for 2 h and (BiT45C4) (e) 930^0C for 2 h (BiT45C5).

Fig. 8. Secondary electron FESEM images showing the microstructures of the glass-ceramics derived from BiT45 glass heat-treated at (a) 580^0C for 1 h (BiT45C1), (b) 10 h (BiT45C2) and (c) EDS spectra of spherical grains, black arrow indicates the grain on which the spectra was taken.

Fig. 9. TEM image showing the microstructure of the BiT45C2 glass-ceramics heat-treated at 580^0C for 10 h (in set at right hand upper corner shows the SAED pattern).

Fig. 10. (Color online) Fourier transformed infrared reflectance spectra of samples BiT20, BiT40 and BiT50. Inset shows variation of Si-O band positions and its reflectivity as a function of BiT content in the glasses.

Fig. 11. Dielectric constant of the glasses BiT10, BiT20, BiT30, BiT40, BiT45, BiT50 and glass-ceramics BiT45C1 and BiT45C2 as a function of BiT content.

Table 1

Physical properties of glasses

Sample	d ($g.cm^{-3}$)	CTE, α ($50\text{-}350^0C$) x 10^{-7} K^{-1}	T_g (^0C)	T_d (^0C)	T_s (^0C)
BiT10	3.00	-	-	-	596
BiT20	3.36	150	479	519	571
BiT30	3.82	143	462	498	544
BiT40	4.46	132	456	487	528
BiT45	4.70	130	455	485	527
BiT50	4.92	129	452	484	526

d, density; α, coefficient of thermal expansion (CTE); T_g, glass transition temperature; T_d, dilatometric deformation temperature; T_s, softening temperature